THE JOURNAL OF PHYSICAL CHEMISTRY A

Article

pubs.acs.org/JPCA

Gaussian Binning of the Vibrational Distributions for the Cl + $CH_4(v_{4/2} = 0, 1) \rightarrow H + CH_3Cl(n_1n_2n_3n_4n_5n_6)$ Reactions

Gábor Czakó*

Laboratory of Molecular Structure and Dynamics, Institute of Chemistry, Eötvös University, H-1518 Budapest 112, P.O. Box 32, Hungary

ABSTRACT: We test several binning techniques to obtain mode-specific final-state distributions for polyatomic reactions. Normal mode analysis is done after an exact transformation to the Eckart frame. Standard histogram binning (HB) and three different variants of the energy-based Gaussian binning (1GB) are employed to obtain the probabilities of the vibrational states. We consider the two major issues of the polyatomic quasiclassical product analysis, i.e., (1) rounding the classical action to the nearest integer can result in unphysical states and (2) the normal-mode analysis can break down for highly distorted geometries. We show that 1GB can handle issue 1 when the total vibrational energy is evaluated in the normal mode space using the harmonic approximation and both issues 1 and 2 can be solved when the total vibrational energy is calculated exactly in the Cartesian space. We found that anharmonicity in the quantized energy levels does not have a significant effect on the final-state distributions. Quasiclassical trajectory calculations are performed for the reactant ground-state and bending-excited $Cl(^2P_{3/2}) + CH_4(v_{4/2} = 0, 1) \rightarrow H + CH_3Cl$ reactions using an ab initio potential energy surface. The product analysis techniques are successfully applied to the CH_3Cl product molecules and some qualitative features of the results are discussed.

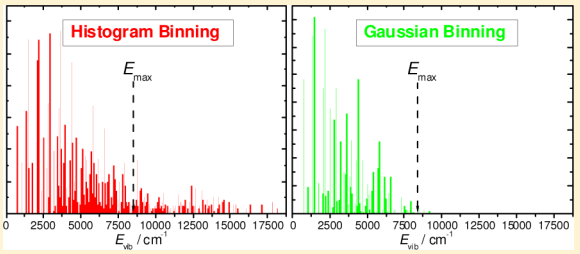

INTRODUCTION

Rigorous quantum dynamics computations are routinely performed nowadays for atom + diatom reactions, providing state-to-state integral and differential cross sections in excellent agreement with experiment.[1,2] Recently, polyatomic processes have received a lot of attention as well.[3−13] State-of-the-art experimental techniques are able to probe specific vibrational states of the polyatomic products, thereby providing deeper insight into the mode-selective dynamics of gas-phase polyatomic chemical reactions.[13,14] The first-principles simulation of these polyatomic reactions provides a considerable challenge to theory, because the rigorous quantum computation of mode-specific final-state distributions for reactions involving more than four atoms is not feasible nowadays.[15] Therefore, the quasiclassical trajectory (QCT) method is frequently used to study the dynamics of polyatomic processes.[3−8,10,11] On the basis of recent method developments, QCT can provide mode-specific vibrational distributions for polyatomic product molecules.[16,17,7] However, due to its classical nature, QCT allows unphysical energy redistribution among the different vibrational modes; therefore, the standard final-state assignments, i.e., histogram binning (HB), can result in nonzero probabilities for energetically not allowed states. To incorporate the "quantum spirit" into the QCT product analysis, the so-called Gaussian binning (GB) procedure was proposed.[18,19] GB assigns a weight for each reactive trajectory favoring the trajectories in which the classical vibrational actions are closer to integer values. This method has been successfully used for diatomic products; however, for polyatomic processes GB was impractical due to the exponential scaling of the computational time with respect to the number of the vibrational modes. In 2009 we proposed[16] a practical method to calculate the weight for N-atomic products using the total vibrational energy instead of the $3N - 6$ vibrational actions. Following Bonnet and Espinosa-García,[20] we call this method 1GB, because it uses only one Gaussian instead of the product of $3N - 6$ Gaussians. The 1GB method has been successfully used in recent studies on the $X + CH_4 \rightarrow HX + CH_3$ (X = F, Cl, O) [refs 16, 6, 21], $(H_2O)_2 \rightarrow 2H_2O$ [ref 22], $OH + D_2 \rightarrow D + HOD$ [refs 23, 24], $OH + CO \rightarrow H + CO_2$ [ref 25], and their isotopologue-analogue reactions.

In the present paper we focus on the reactant ground-state and bending-excited $Cl + CH_4(v_{4/2} = 0, 1) \rightarrow H + CH_3Cl(n_1(a_1)n_2(a_1)n_3(a_1)n_4(e)n_5(e)n_6(e))$ reactions and test the performance of the 1GB method for a five-atomic product molecule. We discuss different approaches to assign normal mode harmonic vibrational quantum numbers for polyatomic products and give the details of a practical implementation used in this study. We also introduce modifications of the 1GB method proposed in ref 16 and compare the vibrational distributions obtained with the different 1GB procedures and also with the standard HB.

MODE-SPECIFIC VIBRATIONAL ANALYSIS FOR POLYATOMIC PRODUCTS

The first step of the product analysis procedure is to relate the final configuration, with Cartesian coordinates denoted by $\mathbf{r}_i$

Received: May 8, 2012
Revised: June 20, 2012
Published: June 21, 2012

(i = 1, 2, ..., N), of the N-atomic product to normal mode displacements of a reference minimum geometry (denoted as $\mathbf{r}_i^{eq}$). There are different ways to find the reference geometry in the Cartesian space. (1) We can initiate a gradient-based geometry optimization procedure from $\mathbf{r}_i$ to locate the closest minimum without introducing significant overall rotation in the Cartesian space. This method can be useful when the minimum energy structure is unknown a priori and/or multiple minima exist on the potential energy surface (PES). This is the case in liquids and solids, where Stillinger and Weber[26] used a steepest descent method to assign configurations to a particular minimum. (2) For smaller systems the relevant minimum energy structure is usually known a priori; thus, one just needs to find the optimal orientation of $\mathbf{r}_i$ with respect to $\mathbf{r}_i^{eq}$. This can be done by (a) finding the best overlap between $\mathbf{r}_i$ and $\mathbf{r}_i^{eq}$ by minimizing

$$\sum_{i=1}^{N} \| \mathbf{C}(\theta, \phi, \psi)\mathbf{r}_i - \mathbf{r}_i^{eq} \|^2 \tag{1}$$

with respect to the three Euler angles or (b) solving

$$\sum_{i=1}^{N} m_i \mathbf{r}_i^{eq} \times (\mathbf{C}(\theta, \phi, \psi)\mathbf{r}_i - \mathbf{r}_i^{eq}) = \mathbf{0} \tag{2}$$

thereby satisfying the rotational Eckart condition.[27] Equation 1, which is usually utilized in crystallography, was used in refs 7, 22, 28, and 29, whereas eq 2 is widely applied in spectroscopic applications, e.g., ref 30. As ref 31 shows, (a) and (b) are closely related problems. When mass-scaled coordinates are used in eq 1, then matrix $\mathbf{C}$ minimizing eq 1 also satisfies the Eckart condition given in eq 2.

Practical Implementation. Because in QCT studies the equilibrium structure of the product molecule is usually known, a practical way to proceed is via (2). A general solution for satisfying eq 2 was reported by Dymarsky and Kudin[32] and here we present our implementation, which could be added to any QCT product analysis code to calculate mode-specific vibrational distributions for polyatomic molecules with N nuclei, whose center-of-mass Cartesian coordinates, center-of-mass Cartesian velocities, and masses are denoted as $\mathbf{r}_i$, $\mathbf{v}_i$, and m_i, (i = 1, 2, ..., N), respectively.

(1) Suppose we know the equilibrium structure of the product molecule in *any* orientation in the center of mass frame (denoted as $\mathbf{r}_i^{eq}$). We perform a normal-mode analysis in $\mathbf{r}_i^{eq}$, which provides, in the case of nonlinear equilibrium structure, $3N - 6$ nonzero harmonic frequencies ω_k and the orthogonal transformation matrix $\mathbf{l} \in \mathcal{R}^{(3N-6)\times 3\times N}$, which transforms from mass-scaled Cartesian coordinates to normal coordinates. This normal-mode analysis is done only *once* at the beginning of the product analysis and the same reference structure and $\mathbf{l}$ matrix are used for every trajectory. For each trajectory $\mathbf{r}_i$ and $\mathbf{v}_i$ are rotated to the Eckart frame corresponding to reference geometry $\mathbf{r}_i^{eq}$. Thus, the steps discussed below must be repeated for each reactive trajectory.

(2) We remove the angular momentum by modifying velocities as

$$\mathbf{v}_i^{nr} = \mathbf{v}_i - \boldsymbol{\Omega} \times \mathbf{r}_i \tag{3}$$

where $\boldsymbol{\Omega} = \mathbf{I}^{-1}\mathbf{j}$, where $\mathbf{I}^{-1}$ is the inverse of the moment of inertia tensor at $\mathbf{r}_i$ and $\mathbf{j} = \sum_{i=1}^{N} \mathbf{r}_i \times (m_i \mathbf{v}_i)$.

(3) The matrix $\mathbf{C}$ which transforms to the Eckart frame is obtained as follows:

$$A_{n,m} = \sum_{i=1}^{N} m_i r_{i,n} r_{i,m}^{eq} \qquad n, m = 1(x), 2(y), 3(z) \tag{4}$$

$$\mathbf{A}_1 = \mathbf{A}\mathbf{A}^T \quad \text{and} \quad \mathbf{A}_2 = \mathbf{A}^T\mathbf{A} \tag{5}$$

$$\mathbf{C} = \mathbf{U}_1\mathbf{U}_2^T \tag{6}$$

where the columns of $\mathbf{U}_1$ and $\mathbf{U}_2$ contain the normalized eigenvectors of the real symmetric matrices $\mathbf{A}_1$ and $\mathbf{A}_2$, respectively. The Cartesian coordinates, which exactly satisfy the Eckart conditions and the corresponding velocities are obtained as $\mathbf{C}\mathbf{r}_i$ and $\mathbf{C}\mathbf{v}_i^{nr}$, respectively. Before we move forward, it is important to consider the fact that the sign of an eigenvector is not well-defined; therefore, eight different $\mathbf{C}$ matrices exist, which all satisfy the Eckart conditions. The $\mathbf{C}$ matrix of interest is obtained by constructing all the eight matrices as

$$\mathbf{C}^{\mathbf{a}} = \mathbf{U}_1^{\mathbf{a}}\mathbf{U}_2^T \tag{7}$$

where

$$(\mathbf{U}_1^{\mathbf{a}})_{n,m} = (-1)^{a_m}(\mathbf{U}_1)_{n,m} \qquad \mathbf{a} = (a_1, a_2, a_3)$$
$$a_1 = 1, 2 \qquad a_2 = 1, 2 \qquad a_3 = 1, 2 \tag{8}$$

and we find the minimum of $\sum_{i=1}^{N} \|\mathbf{C}^{\mathbf{a}}\mathbf{r}_i - \mathbf{r}_i^{eq}\|^2$ with respect to $\mathbf{a} = (a_1, a_2, a_3)$. Hereafter, let us denote the transformation matrix that gives the best overlap between $\mathbf{C}^{\mathbf{a}}\mathbf{r}_i$ and $\mathbf{r}_i^{eq}$ as $\mathbf{C}$.

(4) The normal coordinates are obtained as

$$Q_k = \sum_{i=1}^{N} \sqrt{m_i}\mathbf{l}_{ki}\Delta\mathbf{r}_i \qquad k = 1, 2, ..., 3N - 6 \tag{9}$$

where $\Delta\mathbf{r}_i = \mathbf{C}\mathbf{r}_i - \mathbf{r}_i^{eq}$ and similarly the momenta in the normal coordinate space are

$$P_k = \sum_{i=1}^{N} \sqrt{m_i}\mathbf{l}_{ki}\mathbf{C}\mathbf{v}_i^{nr} \qquad k = 1, 2, ..., 3N - 6 \tag{10}$$

(5) The harmonic vibrational energy for each normal mode is calculated as

$$E_k = \frac{P_k^2}{2} + \frac{\omega_k^2 Q_k^2}{2} \qquad k = 1, 2, ..., 3N - 6 \tag{11}$$

(6) A noninteger classical harmonic action for each mode is obtained as

$$n_k' = \frac{E_k}{\omega_k} - \frac{1}{2} \qquad k = 1, 2, ..., 3N - 6 \tag{12}$$

The integer vibrational quanta are assigned to quantum states by rounding n_k' to the nearest integer value n_k. Hereafter we denote a vibrational state $(n_1, n_2, ..., n_{3N-6})$ as $\mathbf{n}$. We note that some of the above steps are similar to those of previous studies.[16,17] The main difference between the above procedure and the method of ref 16 is in steps (1) and (3), where the present implementation is more efficient and robust.

Binning Techniques. The standard QCT studies apply the HB technique, where the probability of a particular vibrational state $\mathbf{n}$ is

$$P_{HB}(\mathbf{n}) = \frac{N(\mathbf{n})}{N_{traj}} \tag{13}$$

where $N(\mathbf{n})$ is the number of products in state $\mathbf{n}$ from the total number of trajectories N_{traj}.

dx.doi.org/10.1021/jp3044797 | J. Phys. Chem. A 2012, 116, 7467−7473

Using the 1GB approach a Gaussian weight is defined for each product as

$$G_p(\mathbf{n}) = \frac{\beta}{\sqrt{\pi}} e^{-\beta^2\{[E(\mathbf{n}'_p)-E(\mathbf{n})]/2E(\mathbf{0})\}^2}$$
$$p = 1, 2, ..., N(\mathbf{n}) \quad (14)$$

where $\beta = 2(\ln 2)^{1/2}/\delta$, δ is the full-width at half-maximum, and $E(\mathbf{0})$ is the harmonic zero-point energy (ZPE). Then, the probability of $\mathbf{n}$ can be obtained as

$$P_{GB}(\mathbf{n}) = \frac{\sum_{p=1}^{N(\mathbf{n})} G_p(\mathbf{n})}{N_{traj}} \quad (15)$$

In this study we consider three different ways to calculate $G_p(\mathbf{n})$ by using different approaches to get the energies $E(\mathbf{n}'_p)$ and $E(\mathbf{n})$ used in eq 14.

(1) As we proposed originally in 2009,[16] one can use the harmonic energy formulas for both $E(\mathbf{n}'_p)$ and $E(\mathbf{n})$ as follows:

$$E(\mathbf{n}'_p) = \sum_{k=1}^{3N-6} \omega_k \left(n'_{k,p} + \frac{1}{2}\right) \quad (16)$$

and

$$E(\mathbf{n}) = \sum_{k=1}^{3N-6} \omega_k \left(n_k + \frac{1}{2}\right) \quad (17)$$

As we showed recently in the case of the fragments of the water dimer,[22] a possible issue of this approach is that the harmonic normal mode approximation may fail at highly distorted configurations and, thus, $E(\mathbf{n}'_p)$ may be seriously overestimated.

(2) One can also determine $E(\mathbf{n}'_p)$ exactly in the Cartesian space as

$$E(\mathbf{n}'_p) = \frac{1}{2}\sum_{i=1}^{N} m_i \mathbf{v}_{i,p}^{nr}(\mathbf{v}_{i,p}^{nr})^T + V(\mathbf{r}_{1,p}, \mathbf{r}_{2,p}, ..., \mathbf{r}_{N,p}) - V(\mathbf{r}_1^{eq}, \mathbf{r}_2^{eq}, ..., \mathbf{r}_N^{eq}) \quad (18)$$

where $\mathbf{v}_{i,p}^{nr}$ is the velocity of the pth product corresponding to zero angular momentum as defined in eq 3 and V is the potential energy of the N-atomic product. This second approach uses eqs 18 and 17 for $E(\mathbf{n}'_p)$ and $E(\mathbf{n})$, respectively.

(3) Here we propose to incorporate the effect of vibrational anharmonicity by using the second-order vibrational perturbation theory (VPT2) to calculate $E(\mathbf{n})$ as

$$E(\mathbf{n}) = \sum_{k=1}^{3N-6} \omega_k \left(n_k + \frac{1}{2}\right) + \sum_{k\geq l}^{3N-6} \chi_{k,l}\left(n_k + \frac{1}{2}\right)\left(n_l + \frac{1}{2}\right) \quad (19)$$

where $\chi_{k,i}$ are the anharmonicity constants, which can be nowadays obtained routinely by ab initio program packages. Now we can calculate the weight from the anharmonic energies $E(\mathbf{n}'_p)$ and $E(\mathbf{n})$ utilizing eqs 18 and 19, respectively.

Hereafter we denote 1GB approaches (1), (2), and (3) as GB(harm), GB(harm-exact), and GB(aharm-exact), respectively.

COMPUTATIONAL DETAILS

We have performed QCT calculations for the reactant ground-state and bending-excited $Cl(^2P_{3/2}) + CH_4(v_{4/2} = 0, 1) \rightarrow H + CH_3Cl$ reactions using a full-dimensional ab initio global PES. The PES was first reported in ref 5, and a detailed description can be found in ref 6. The PES accurately describes both the abstraction and substitution channels, in the present study we focus on the latter. Standard normal mode sampling was applied to prepare the initial states $CH_4(v = 0)$, $CH_4(v_4 = 1)$, and $CH_4(v_2 = 1)$, where the harmonic frequencies (corresponding to the PES) of the $v_4(t_2)$ and $v_2(e)$ bending modes are 1355 and 1560 cm^{-1}, respectively.[6] The relative orientation of the reactants was randomly sampled and the initial distance was set to $(x^2 + b^2)^{1/2}$, where b is the impact parameter and x = 10 bohr. b was scanned from 0 to 7 bohr with a step size of 0.5 or 0.25 bohr. (Note that for the substitution channel the maximum b is only about 2 bohr. The wider b range applied in this study can describe the abstraction reaction as well.) We have performed computations at collision energies (E_{coll}) of 12 000, 14 000, 16 000, 18 000, 20 000 cm^{-1} and run 5000 trajectories at each b using 0.0726 fs integration step. At E_{coll} of 14 000 and 16 000 cm^{-1} we scanned b with a smaller step size of 0.25 bohr, because we report the most detailed product analyses at these E_{coll}.

The mode-specific product-state distributions for CH_3Cl have been computed using the different techniques described in the former section. For 1GB we used a Gaussian function with δ = 0.1. The anharmonicity constants shown in eq 19 were computed

Table 1. Harmonic and Anharmonic Zero-Point Energies and Vibrational Fundamentals (cm^{-1}) of CH_3Cl

	ω^a	Δv^b	v^c
ZPE	8231 (8318)	−115	8116 (8203)
$\nu_3(a_1)$	730 (737)	−16	714 (721)
$\nu_6(e)$	1034 (1039)	−21	1013 (1018)
$\nu_2(a_1)$	1358 (1390)	−34	1324 (1356)
$\nu_5(e)$	1502 (1500)	−44	1458 (1456)
$\nu_1(a_1)$	2972 (3076)	−103	2869 (2973)
$\nu_4(e)$	3165 (3178)	−139	3026 (3039)

[a]Harmonic results corresponding to the PES of refs 5 and 6. In parentheses the CCSD(T)/aug-cc-pVTZ results are given. [b]Anharmonic contributions obtained by VPT2 at the MP2/aug-cc-pVTZ ab initio level of theory. [c]Anharmonic results obtained as $\omega + \Delta v$.

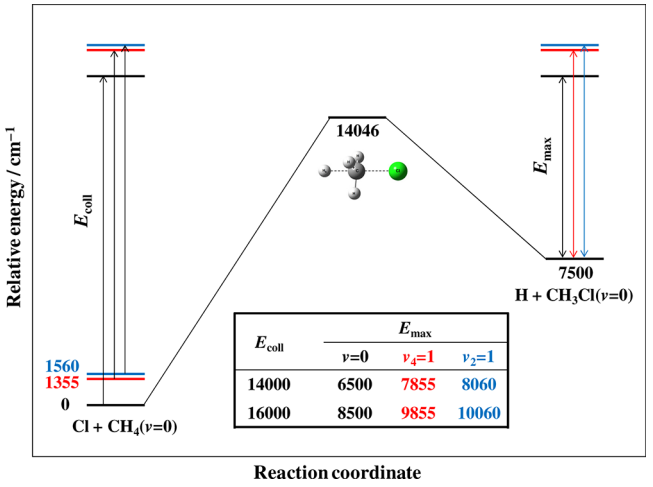

Figure 1. Schematic of the vibrationally adiabatic potential energy surface of the $Cl(^2P_{3/2}) + CH_4(v_{4/2} = 0, 1) \rightarrow H + CH_3Cl$ reactions showing the collision energy (E_{coll}) dependence of the maximal available internal energy (E_{max}) for CH_3Cl at different initial states of the reactant. The relative energies correspond to the global PES of refs 5 and 6 including harmonic zero-point energy corrections.

dx.doi.org/10.1021/jp3044797 | J. Phys. Chem. A 2012, 116, 7467−7473

by the ab initio package CFOUR[33] using VPT2 at the MP2/aug-cc-pVTZ level of theory. Note that in eq 19 we used ω_k corresponding to the PES and just $\chi_{k,i}$ were taken from direct ab initio computations. Test computations showed that the final results are not sensitive to the ab initio level employed. The harmonic and anharmonic fundamental frequencies of CH_3Cl are given in Table 1.

RESULTS AND DISCUSSION

A schematic of the vibrationally adiabatic PES of the $Cl(^2P_{3/2}) + CH_4(v = 0) \rightarrow H + CH_3Cl(v = 0)$ reaction is shown in Figure 1. The ground-state adiabatic barrier height is 14 046 cm^{-1}, well below the classical value of 15 061 cm^{-1}.[5,6] The reaction enthalpy (ΔH_0°) is 7500 cm^{-1}, again significantly less than the vibrationless endothermicity of 9087 cm^{-1}.[5,6] (All the above energies correspond to the PES). The reaction enthalpy determines the maximum available internal energy (E_{max}) for CH_3Cl as $E_{coll} - \Delta H_0^\circ + E_{int}(CH_4)$, where $E_{int}(CH_4)$ is the internal energy of CH_4 relative to the ZPE, i.e., 0, 1355, and 1560 cm^{-1} for $CH_4(v = 0)$, $CH_4(v_4 = 1)$, and $CH_4(v_2 = 1)$, respectively. Because the atomic product (H atom) cannot violate ZPE, even the classical QCT method cannot produce CH_3Cl with an internal energy larger than E_{max}. However, we can still compute nonzero probabilities for those vibrational states of CH_3Cl that have energy larger than E_{max}. This can happen due to the following reasons: (1) Because the assignment of the vibrational quantum numbers is based on rounding to the nearest integer, the upper limit of $E(\mathbf{n}) - E(\mathbf{n}')$ is as high as the ZPE. (2) The normal-mode analysis can break down for highly distorted geometries resulting in an unphysical increase in the mode energies. It is clear the 1GB approach can deal with issue 1, because large deviations between $E(\mathbf{n})$ and $E(\mathbf{n}')$ result in small weights. Can 1GB handle issue 2 as well? Do these issues result in a complete breakdown of the

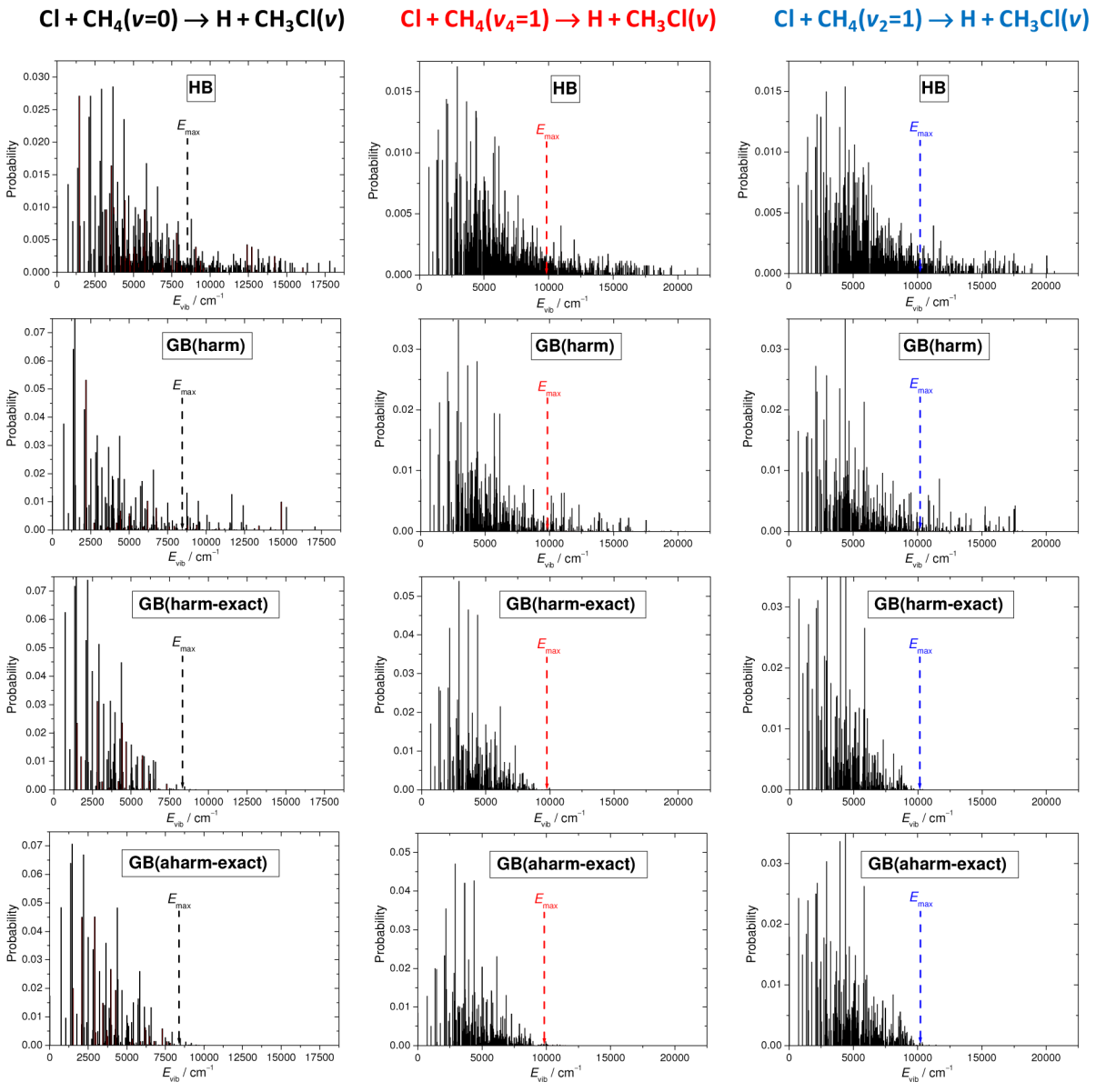

Figure 2. Product vibrational distributions (showing all the product states) for the $Cl(^2P_{3/2}) + CH_4(v_{4/2} = 0, 1) \rightarrow H + CH_3Cl(v)$ reactions at collision energy of 16 000 cm^{-1} obtained by different binning techniques as described in the text. The vibrational energy is relative to the ZPE of CH_3Cl, and E_{max} indicates the maximum available internal energy.

dx.doi.org/10.1021/jp3044797 | J. Phys. Chem. A 2012, 116, 7467−7473

standard HB method? We seek answers for these questions by analyzing the CH_3Cl product molecules of the title reaction.

Vibrational distributions of CH_3Cl at E_{coll} = 16 000 cm^{-1} obtained by HB and three different variants of 1GB are shown in Figure 2. The E_{max} values are 8500, 9855, and 10 060 cm^{-1} for reactants $CH_4(v = 0)$, $CH_4(v_4 = 1)$, and $CH_4(v_2 = 1)$, respectively. HB, however, shows substantial populations above E_{max} up to about 18 000, 20 000, and 20 000 cm^{-1}, respectively. (Note that the CH_3 stretching modes are usually in the ground state or have one quantum excitation. The overtones and combinations of the low frequency modes have significant populations above E_{max}.) This is clearly a failure of HB due to issues 1 and/or 2. GB(harm) improves the results because the populations and the density of the states decrease above E_{max}; however, we still get many states with significant populations at the physically not allowed region. The improvement over HB is due to the fact that GB(harm) effectively handles issue 1; however, GB(harm) cannot solve issue 2, i.e., the overestimation of $E(\mathbf{n}')$ due to the failure of the normal-mode analysis. In the traditional mode-based GB approach there is no possibility to overcome this issue. Fortunately, 1GB offers a practical way to compensate the possible breakdown of the normal-mode analysis, because 1GB only requires the total classical vibrational energy of the product, which can be computed exactly in the Cartesian space as shown in eq 18. When we use either GB(harm-exact) or GB(aharm-exact), which calculates the weight by comparing $E(\mathbf{n})$ and the exactly determined $E(\mathbf{n}')$, the states above E_{max} completely vanish. Significant qualitative differences between the GB(harm-exact) and GB(aharm-exact) distributions are not seen, indicating that a harmonic approximation for $E(\mathbf{n})$ is satisfactory in QCT product analyses. However, the normal-mode analysis can fail in some cases when the actual geometry is highly distorted; thus, $E(\mathbf{n}')$ can be seriously overestimated, when it is determined in the normal mode space. This can especially be expected for the title reaction, because it produces vibrationally hot CH_3Cl molecules. As Figure 2 shows, most of the CH_3Cl molecules are vibrationally excited and the distributions peak around 2000−3000 and 3000−5000 cm^{-1} for the ground-state and bending-excited reactions, respectively. We note that only a few trajectories violate the ZPE of CH_3Cl (see ref 6); thus, the ZPE-constrained results would be similar to the present ones. In summary, both GB(harm-exact) and GB(aharm-exact) provide mode-specific distributions satisfying the energy requirements and these advanced 1GB methods greatly improve the standard HB results.

In Figure 3 the distributions of the $CH_3Cl(00n_300)$ states are shown at E_{coll} = 14 000 cm^{-1} obtained by the four different binning methods. (n_3 denotes the vibrational quanta on the lowest-frequency mode, i.e., CCl stretch.) For the Cl + $CH_4(v = 0)$ reaction GB(harm-exact) and GB(aharm-exact) show that vibrational states up to v_3 = 5 are populated, whereas GB(harm) and especially HB allow excitations up to v_3 = 11. The population of $CH_3Cl(v = 0)$ is small, most of the products are formed in v_3 = 2 and 3. When the reactant bending mode is excited, the product vibrational distributions are hotter and broader with significant populations for v_3 = 1−6 and v_3 = 0−7 for Cl + $CH_4(v_4 = 1)$ and $CH_4(v_2 = 1)$, respectively. Because the distributions are normalized over all the product states, we can observe that GB methods provide more pronounced probabilities for the overtones than HB does. In other words, when one uses HB, the internal energy is spread among many states showing smaller probabilities for specific vibrational states.

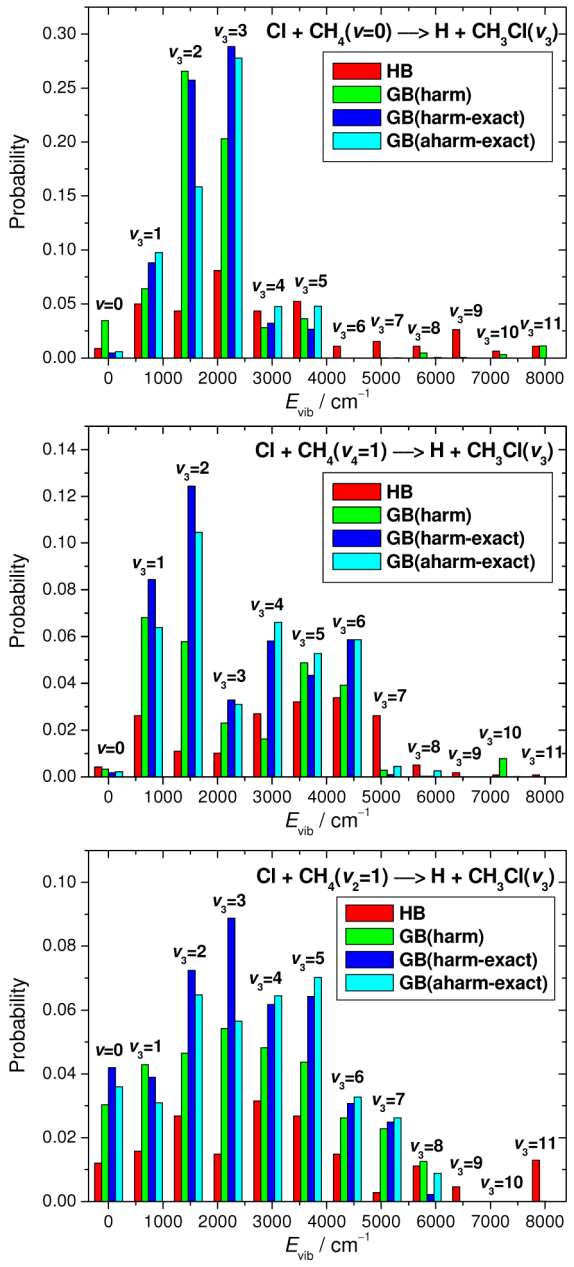

Figure 3. Populations of the C−Cl stretching mode (v_3) excited products for the $Cl(^2P_{3/2})$ + $CH_4(v_{4/2}$ = 0, 1) → H + $CH_3Cl(v_3)$ reactions at collision energy of 14 000 cm^{-1} obtained by different binning techniques as described in the text. The probabilities are normalized over all the product states, whereas here only the $(00n_300)$ states are shown.

Cross section ratios (σ_b/σ_g) between the reactant bending-excited (v_4 = 1 or v_2 = 1, but the results are similar) and ground-state reactions are shown in Figure 4 in the E_{coll} = 12 000−20 000 cm^{-1} range obtained by the different binning techniques. (Note that in the case of the total cross sections HB means no binning; i.e., all the reactive trajectories are considered with equal weights.) As seen in Figure 4, the bending excitations enhance the reaction substantially especially at the threshold region. At this region HB and GB provide significantly different results, because the σ_b/σ_g ratios are much larger when GB is employed. At E_{coll} = 12 000 cm^{-1}, well below the adiabatic barrier height, we found some reactive Cl + $CH_4(v = 0)$ → H + CH_3Cl trajectories;

dx.doi.org/10.1021/jp3044797 | J. Phys. Chem. A 2012, 116, 7467−7473

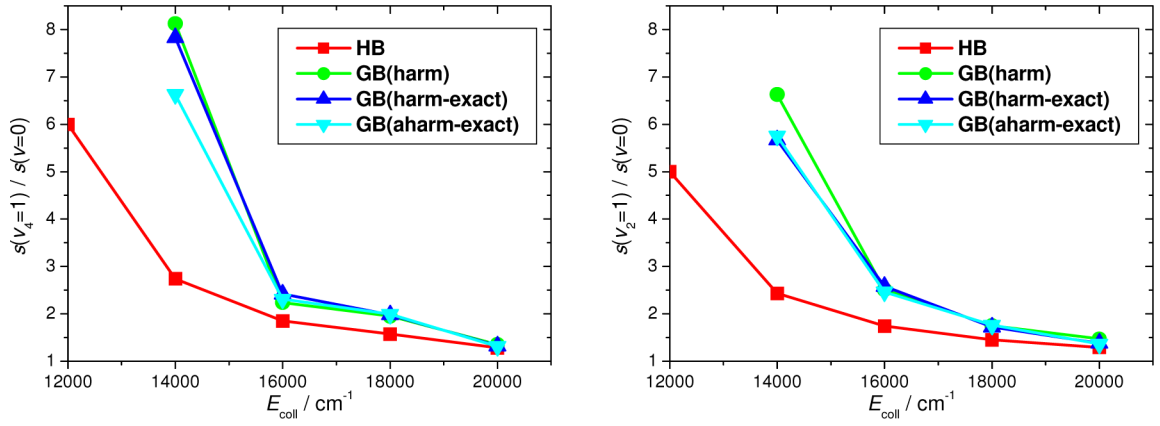

Figure 4. Cross section ratios for the reactant bending excited vs ground state $Cl(^2P_{3/2}) + CH_4 \rightarrow H + CH_3Cl$ reactions as a function of collision energy obtained by different binning techniques as described in the text.

however, GB gives zero weight to these trajectories, which could be obtained due to some unphysical internal energy redistribution, a well-known issue of the QCT method. At an E_{coll} close to the adiabatic barrier height (14 000 cm^{-1}), HB and GB provide σ_b/σ_g ratios of about 2−3 and 6−8, respectively, whereas at as high E_{coll} as 20 000 cm^{-1}, the σ_b/σ_g ratios are about 1.2−1.5 in the cases of both HB and GB. For the ratios of the total cross sections the various 1GB approaches, i.e., GB(harm), GB(harm-exact), and GB(aharm-exact), result in similar ratios, which can be quite different from the standard HB results in the threshold region.

SUMMARY AND CONCLUSIONS

We have investigated several strategies that move beyond the standard quasiclassical product analysis. The methods were applied to the CH_3Cl product obtained by the substitution reaction of ground-state and bending-excited CH_4 with Cl atom. Because CH_3Cl has a well-known equilibrium structure, one just needs to find a transformation, which rotates the final distorted configuration to the Eckart frame defined by the equilibrium geometry. We presented the details of a practical implementation of such a transformation. We also considered three different variants of the energy-based 1GB method to obtain mode-specific vibrational populations. Although 1GB always improves the results of the standard HB method, we showed that the original implementation of 1GB as proposed by us[16] in 2009 cannot deal with the possible breakdown of the normal-mode analysis occurring at highly distorted geometries. Nevertheless, 1GB offers a solution of this issue by calculating the total vibrational energy $[E(\mathbf{n}')]$ exactly in the Cartesian space. When one calculates the Gaussian weight by comparing the quantized energy level $[E(\mathbf{n})]$ of the given state to this exact vibrational energy of the product, the results significantly improve and all the states get zero probabilities, which are expected to be closed on the basis of the available energy. Our numerical results show that anharmonicity in $E(\mathbf{n})$ does not have a significant effect on the product-state distributions. Therefore, for practical applications we propose to use 1GB, where the weight is obtained from harmonic $E(\mathbf{n})$ (eq 17) and exact $E(\mathbf{n}')$ (eq 18).

The normal-mode analysis method and the binning techniques described in this paper could be straightforwardly implemented for any quasiclassical product analysis code. Here, we successfully used the method for CH_3Cl and we expect many additional applications in the near future even for much larger systems.

AUTHOR INFORMATION

Corresponding Author

*E-mail: czako@chem.elte.hu.

Notes

The author declares no competing financial interest.

ACKNOWLEDGMENTS

The author thanks the Scientific Research Fund of Hungary (OTKA, NK83583) and the European Union and the European Social Fund (TÁMOP-4.2.1/B-09/1/KMR-2010-0003) for financial support. Discussions with Prof. Joel Bowman, Prof. Attila Császár, Dr. Edit Mátyus, and Mr. Csaba Fábri are gratefully acknowledged.

REFERENCES

(1) Clary, D. C. *Science* **2008**, *321*, 789−791.
(2) Che, L.; Ren, Z.; Wang, X; Dong, W.; Dai, D.; Wang, X.; Zhang, D. H.; Yang, X.; Sheng, L.; Li, G.; et al. *Science* **2007**, *317*, 1061−1064.
(3) Czakó, G.; Shepler, B. C.; Braams, B. J.; Bowman, J. M. *J. Chem. Phys.* **2009**, *130*, 084301.
(4) Czakó, G.; Bowman, J. M. *J. Am. Chem. Soc.* **2009**, *131*, 17534−17535.
(5) Czakó, G.; Bowman, J. M. *Science* **2011**, *334*, 343−346.
(6) Czakó, G.; Bowman, J. M. *J. Chem. Phys.* **2012**, *136*, 044307.
(7) Greaves, S. J.; Rose, R. A.; Abou-Chahine, F.; Glowacki, D. R.; Troya, D.; Orr-Ewing, A. J. *Phys. Chem. Chem. Phys.* **2011**, *13*, 11438−11445.
(8) Castillo, J. F.; Aoiz, F. J.; Banares, L. *J. Chem. Phys.* **2006**, *125*, 124316.
(9) Mikosch, J.; Trippel, S.; Eichhorn, C.; Otto, R.; Lourderaj, U.; Zhang, J. X.; Hase, W. L.; Weidemüller, M.; Wester, R. *Science* **2008**, *319*, 183−186.
(10) Troya, D.; Pascual, R. Z.; Schatz, G. C. *J. Phys. Chem. A* **2003**, *107*, 10497−10506.
(11) Hu, W.; Lendvay, G.; Troya, D.; Schatz, G. C.; Camden, J. P.; Bechtel, H. A.; Brown, D. J. A.; Martin, M. R.; Zare, R. N. *J. Phys. Chem. A* **2006**, *110*, 3017−3027.
(12) Yoon, S.; Holiday, R. J.; Crim, F. F. *J. Phys. Chem. B* **2005**, *109*, 8388−8392.
(13) Yan, S.; Wu, Y.-T.; Zhang, B.; Yue, X.-F.; Liu, K. *Science* **2007**, *316*, 1723−1726.
(14) Rocher-Casterline, B. E.; Ch'ng, L. C.; Mollner, A. K.; Reisler, H. *J. Chem. Phys.* **2011**, *134*, 211101.
(15) Xiao, C.; Xu, X.; Liu, S.; Wang, T.; Dong, W.; Yang, T.; Sun, Z.; Dai, D.; Xu, X.; Zhang, D. H.; et al. *Science* **2011**, *333*, 440−442.
(16) Czakó, G.; Bowman, J. M. *J. Chem. Phys.* **2009**, *131*, 244302.

(17) Corchado, J. C.; Espinosa-García, J. *Phys. Chem. Chem. Phys.* **2009**, *11*, 10157−10164.
(18) Bonnet, L.; Rayez, J. C. *Chem. Phys. Lett.* **1997**, *277*, 183−190.
(19) Bonnet, L.; Rayez, J. C. *Chem. Phys. Lett.* **2004**, *397*, 106−109.
(20) Bonnet, L.; Espinosa-García, J. *J. Chem. Phys.* **2010**, *133*, 164108.
(21) Czakó, G.; Bowman, J. M. *Proc. Natl. Acad. Sci. U. S. A.* **2012**, *109*, 7997−8001.
(22) Czakó, G.; Wang, Y.; Bowman, J. M. *J. Chem. Phys.* **2011**, *135*, 151102.
(23) Sierra, J. D.; Bonnet, L.; González, M. *J. Phys. Chem. A* **2011**, *115*, 7413−7417.
(24) Bonnet, L.; Espinosa-García, J.; Corchado, J. C.; Liu, S.; Zhang, D. H. *Chem. Phys. Lett.* **2011**, *516*, 137−140.
(25) García, E; Corchado, J. C.; Espinosa-García, J. *Comput. Theor. Chem.* **2012**, *990*, 47−52.
(26) Stillinger, F. H.; Weber, T. A. *Science* **1984**, *225*, 983−989.
(27) Eckart, C. *Phys. Rev.* **1935**, *47*, 552−558.
(28) Czakó, G.; Kaledin, A. L.; Bowman, J. M. *J. Chem. Phys.* **2010**, *132*, 164103.
(29) Czakó, G.; Kaledin, A. L.; Bowman, J. M. *Chem. Phys. Lett.* **2010**, *500*, 217−222.
(30) Szidarovszky, T.; Fábri, C.; Császár, A. G. *J. Chem. Phys.* **2012**, *136*, 174112.
(31) Kudin, K. N.; Dymarsky, A. Y. *J. Chem. Phys.* **2005**, *112*, 224105.
(32) Dymarsky, A. Y.; Kudin, K. N. *J. Chem. Phys.* **2005**, *112*, 124103.
(33) CFOUR, a quantum chemical program package written by J. F. Stanton, J. Gauss, M. E. Harding, and P. G. Szalay, with contributions from A. A. Auer et al. For the current version, see http://www.cfour.de.